Microporous and Mesoporous Materials 224 (2016) 51–57

Contents lists available at ScienceDirect

Microporous and Mesoporous Materials

journal homepage: www.elsevier.com/locate/micromeso

Phosphate removal from solution by composite of MCM-41 silica with rice husk: Kinetic and equilibrium studies

Moaaz K. Seliem [a], Sridhar Komarneni [b, *], Mostafa R. Abu Khadra [a]

[a] Geology Department, Faculty of Science, Beni-Suef University, Egypt
[b] Department of Ecosystem Science and Management, Materials Research Laboratory, Materials Research Institute, The Pennsylvania State University, University Park, PA 16802, USA

ARTICLE INFO

Article history:
Received 30 August 2015
Received in revised form
31 October 2015
Accepted 6 November 2015
Available online 14 November 2015

Keywords:
Phosphate uptake
Rice husk composite
MCM-41
Adsorption kinetics
Adsorption isotherms

ABSTRACT

Composite of MCM-41 silica with rice husk was synthesized under hydrothermal conditions using cetyltrimethylammonium bromide (CTAB) as an organic template, aqueous ammonia solution (NH_4OH) and rice husk. Rice husk served as not only a silica source but also as a substrate for the deposition of MCM-41. The synthetic hybrid composites were characterized by powder X-ray diffraction (XRD), scanning electron microscope (SEM) and transmission electron microscope (TEM) and tested as sorbents for phosphate from aqueous solution. Kinetic data and equilibrium uptake isotherms were measured. The effects of different experimental parameters such as contact time, initial phosphate concentration, solution pH, adsorbent mass, and the presence of competitive ions on phosphate uptake were investigated. The phosphate uptake kinetics were found to be fast and equilibrium was achieved after 30 min. The phosphate uptake was found to be highly pH dependent. Studies on the effects of competing ions, without keeping the initial pH constant, indicated that phosphate uptake and K_d values decreased in the presence of CO_3^{2-} and NO_3^-, but SO_4^{2-} ions showed little or no effect. With keeping the initial pH constant at 6, the presence of these competing ions had no clear effect on the uptake of phosphate. The phosphate uptake by composite of rice husk with MCM-41 could be described well by the Langmuir isotherm equation. Adsorption kinetic data correlated well with pseudo-second-order model, which suggested that the uptake process might be chemical sorption.

1. Introduction

Human activities related to mining, agriculture and other industries lead to releasing dissolved nutrients such as phosphorous in aquatic environments [1]. Phosphate with a concentration above 0.02 mg/L can be considered as an important factor that causes eutrophication of water bodies [2]. Eutrophication is a process by which a body of water becomes enriched in dissolved nutrients which stimulate the growth of aquatic plants and algae. It affects water quality through the lack of dissolved oxygen level which frequently causes environmental problems such as fish kills, phytoplankton blooms and disturbs the balance of organisms present in water [3,4]. In some regions of the world, more than 40% of water bodies are considered to have eutrophication problems [5]. In Egypt, eutrophication is the principal water quality problem in the most common water bodies such as Manzala, Mariout, Burullus and Qaroun lakes [6,7].

The removal of phosphorus from natural water bodies is essential in the control of eutrophication and therefore, a large number of natural and synthetic materials were tested in the uptake of phosphate from water such as calcite [8], calcium-rich sepiolite [9], kaolinite [10], thermally treated natural playgorskite [11], Tunisian clays minerals and synthetic zeolite [12], activated carbon fiber loaded with lanthanum oxide [1], fly ash [13], porous MgO-biochar nanocomposites [14], ammonium-functionalized MCM-48 [15], mesoporous rodlike $NiFe_2O_4$ [16], natural and surface modified coir pith [17], ferric sludge [3], zirconia-functionalized graphite oxide [18], Al-pillared smectites and mica [19], and Mg–Al layered double hydroxide [20].

Rice husk (RH) is an organic agricultural waste material produced as a byproduct from the rice milling operations. Rice husk is composed of about 50% cellulose, 25–30% lignin and 15–20% of silica [21]. Rice husk is widely used in many industrial applications due to its chemical stability, high mechanical strength, insolubility

* Corresponding author.
E-mail address: komarneni@psu.edu (S. Komarneni).

http://dx.doi.org/10.1016/j.micromeso.2015.11.011
1387-1811/

in water, and its local availability at almost no cost. Untreated and treated rice husks were used in the synthesis of new porous materials such as mesoporous carbons [22], ZSM-5 zeolite [23], ZSM-5 zeolite/porous carbon composite [24], MCM-22 zeolite [25], molded micro- and mesoporous carbon/silica composite [26], Na-A and/or Na-X zeolite/porous carbon composites [27]. Composites of rice husks with MCM-41 and MCM-48 were recently prepared under hydrothermal conditions and tested for the uptake of perchlorate from aqueous solution by Komarneni's group [28,29]. The results showed that composites of rice husks with MCM-41 exhibited significant uptake capacities for perchlorate in the range of 0.12–0.21 mequiv/g [28,29]. According to the above studies, the uptake of perchlorate by the synthetic rice husk composite with MCM-41 silica was related to both MCM-41 silica and rice husk. The residual positive charge on the cationic surfactant micelles trapped in mesopores of silica was found to be responsible for the perchlorate uptake by MCM-41. In addition, some surfactant was also loaded on to the rice husk due to hydrothermal treatment and therefore, MCM-41 and rice husk, both loaded with surfactant, contributed towards the removal of perchlorate in the synthetic composite [28]. On the other hand, composite of rice husk with MCM-48 showed low capacity for perchlorate uptake (0.094 mequiv/g) as compared to rice husk composite with MCM-41 [29]. Untreated (pure) rice husk is expected to have little or no adsorption of phosphate.

From the estimated annual rice production in developing countries (nearly 500 million tons), nearly 100 million tons of rice husk are available annually for utilization and therefore, the excess amount after local uses has posed disposal problems [30]. To the best of our knowledge, the application of composites of rice husk and mesoporous MCM-41 silica as sorbents for phosphate anion, as well as their sorption behavior and mechanism are not investigated so far. Thus, the main objectives of this work were (a) to synthesize and characterize composite of MCM-41 silica with rice husk and to study their ability to remove phosphate ions from aqueous solution, (b) to study the effects of different experimental parameters such as contact time, initial phosphate concentration, solution pH, adsorbent dose, and the presence of coexisting ions on the adsorption performance and (c) to investigate the adsorption characteristics and the mechanisms of phosphate uptake by fitting the experimental data to different kinetics and isotherms models.

2. Experimental

2.1. Materials

Cetyltrimethylammonium bromide (Aldrich, 99%), ammonia solution, distilled water and rice husk were used as starting materials in the synthesis of composite of MCM-41 silica with rice husk.

2.2. Synthesis of composite of MCM-41 silica with rice husk

Rice husk (RH) was washed several times with distilled water to remove the adhered dust and then dried at 100° C overnight. The dried rice husk was mixed with (3 M) HCl solution in a 500 ml glass beaker with stirring at 100° C for 3 h to remove alkaline impurities. The solution was filtered and the husk was washed repeatedly with distilled water until the filtrate was neutral and then, the husk was dried in an oven at 65 °C overnight. After acid treatment, the dried RH was ground to pass through 300-mesh sieve. To prepare MCM-41 silica on the rice husk, the following procedure was used [28]: A 0.51 g of CTAB was first added to 25 ml H_2O in a Teflon vessel with stirring until it was completely dissolved. Then, 16.34 ml of aqueous ammonia solution was added while stirring for 10 min. To the above solution, 0.75 g of rice husk was added with stirring for 10 min. The measured pH values of the mixtures were adjusted to 10 with 5% of hydrochloric acid. Then, the Teflon vessels were sealed in stainless steel Parr reactors and heated in an oven at 100 °C for 24 h. After hydrothermal treatment, the vessels were cooled down to room temperature. The contents from Teflon vessels were centrifuged to separate solids from solutions. Then, the solid products were washed with distilled water and ethanol several times to remove any remaining soluble salts. The solids were dried in an oven at 65 °C. The dried samples were gently ground and homogenized in an agate mortar with a pestle prior to characterization by different techniques and phosphate uptake studies.

2.3. Sample characterization

X-ray powder diffraction patterns were obtained using a Philips APD-3720 diffractometer with Cu Kα radiation, operated at 20 mA and 40 kV in the 2θ range of 1–10 at a scanning speed of 2° min^{-1}. The morphology and particle size of the rice husk composite with MCM-41 were also characterized by scanning electron microscopy using a field emission scanning electron microscope (JSM-6700F, JEOL, Tokyo, Japan) and by a transmission electron microscope (TEM; Model 2010, JEOL, Tokyo, Japan).

2.4. Isotherms study

Equilibrium studies of phosphate were evaluated using different initial concentrations in the range of 0.5–2.5 mM of $Na_2HPO_4 \cdot 2H_2O$ as follows. Fifty milligrams of rice husk composite with MCM-41 was added to 25 ml of 0.5, 1, 1.5, 2 or 2.5 mM of $Na_2HPO_4 \cdot 2H_2O$ in centrifuge tubes and mixed for 24 h on a shaker. After equilibration, the suspensions were filtrated with 45 μ membrane filters, solids and solutions were separated and the solutions were collected in clean vials. All isotherms experiments were conducted using triplicates. The concentrations of phosphate in all solutions were determined by using a Dionex DX-120 ion chromatograph equipped with an AS40 auto sampler, a DS4 detection stabilizer which used a current of 300 mA and a temperature of 35 °C, a 4-mm AS16 column, a 4 mm AG16 guard column, a 4-mm ASRS 300 suppressor. Ion chromatography vials of 25 μl were used for analyses and the concentration of eluant was 25 mM NaOH with all phosphate analyses.

2.5. Kinetics study

Adsorption kinetic experiments were carried out at room temperature by batch technique as follows: 50 mg of each rice husk composite with MCM-41 was equilibrated with 25 ml of 1 mM $Na_2HPO_4 \cdot 2H_2O$ in centrifuge tubes for 5 min, 30 min, 2 h, 4 h, 8 h and 24 h using a shaker. All kinetics experiments were conducted in triplicates. After equilibration, the suspensions were filtrated with 45 μ membrane filters to separate the solid from liquid phase and the liquids were collected in clean vials. The concentration of phosphate in solutions was determined using Dionex DX-120 ion chromatograph as described above.

2.6. Effect of adsorbent dose

To study the influence of adsorbent mass on the removal of phosphate, different weights in the range of 50–250 mg of composite of MCM-41 silica with rice husk were used. A 25 ml of 1 mM $Na_2HPO_4 \cdot 2H_2O$ was mixed with 50, 100, 150, 200 and 250 mg of adsorbent in centrifuge tubes for 24 h on a shaker. The solids and

solutions were separated by filtration and solutions were collected for analysis of phosphate by Dionex DX-120 ion chromatograph.

2.7. Effect of pH

To investigate the influence of pH on the uptake of phosphate, 25 ml of 1 mM $Na_2HPO_4{\cdot}2H_2O$ was added to 50 mg of the synthetic composite of MCM-41 with rice husk in a centrifuge tube and then stirred for 4 h on a shaker. This step was repeated several times with different pH values ranging from 2 to 10. The tests were carried out by keeping the other experimental conditions constant. Sodium hydroxide solution (0.1 N) and nitric acid solution (0.1 N) were used for pH adjustment. The solids and solutions were separated by filtration and solutions were collected for analysis of phosphate by Dionex DX-120 ion chromatograph.

2.8. Effects of coexisting anions and determination of K_d values

The effect of common coexisting anions in water such as SO_4^{2-} or CO_3^{2-} or NO_3^- on the uptake of phosphate was studied as follows: A 50 mg of composite of MCM-41 with rice husk was equilibrated with 25 ml of 1 mM of $Na_2HPO_4{\cdot}2H_2O$ mixed with 5 mM of Na_2SO_4 or 5 mM of Na_2CO_3 or 5 mM of $NaNO_3$ in three different tubes. The suspensions were mixed for 24 h on a shaker. The solid and solution phases were separated by filtration using a 0.45-μm membrane filter and then, solutions were collected in clean vials for phosphate analysis. The distribution coefficient (K_d) is defined as the ratio of the amount of ion adsorbed per gram of solid to the amount of ion remaining per milliliter of solution and is expressed as milliliters per gram [31]. K_d values were calculated as follows:

$$K_d = \frac{C_0 - C_e}{C_e} \times \frac{V}{m} \quad (1)$$

where C_0 and C_e are the ion concentrations in the initial solution and in the solution after equilibration of perchlorate anions, respectively. V is the volume of solution in (ml) and m is the mass of sorbent (g).

3. Results and discussions

3.1. XRD, SEM and TEM results

Fig. 1 shows the X-ray diffraction patterns of rice husk before and after hydrothermal treatment with cetyltrimethylammonium bromide. As can be seen in Fig. 1a, a broad reflection was detected at the 2θ of 22.5° which is a characteristic peak of amorphous silica. On the other hand, the X-ray diffraction pattern of composite of MCM-41 silica with rice husk was characterized by the presence of low angle peak, which refers to the main reflection (100) of MCM-41 mesoporous silica materials (Fig. 1b). The morphology of MCM-41 composite with rice husk prepared at 100 °C for 24 h is shown in Fig. 2. Silica was extracted from the rice husk during the hydrothermal treatment under alkaline conditions. This silica reacted with cetyltrimethylammonium bromide (CTAB) surfactant to form MCM-41 mesoporous silica material that covered the surface of rice husk as a thin coating [28]. The SEM pictures, under different magnifications, clearly show that the MCM-41 silica material was deposited on the rice husk surface (Fig. 2a and b). At higher magnifications, the morphology of MCM-41 clearly appears as aggregates of wormy and spherical particles (Fig. 2c and d). The hexagonal mesostructure of MCM-41 and its composite with rice husk is shown by TEM image (Fig. 2e). With phosphate adsorption, the morphology of MCM-41 silica with rice husk composite after 30 min of contact time was changed. The surface became rough and irregular with the presence of a broad network and a high open structure (Fig. 2f).

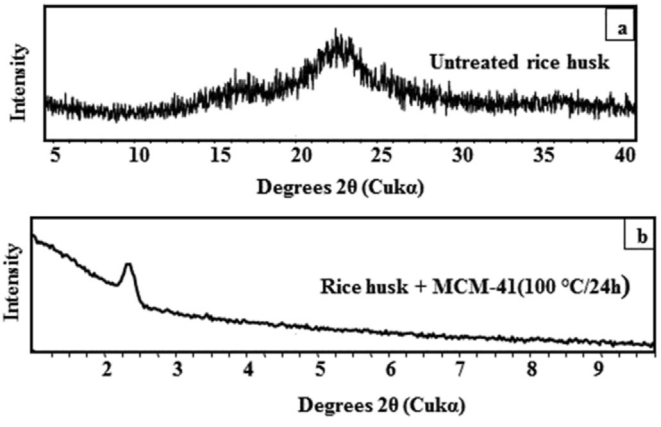

Fig. 1. XRD patterns of (a) untreated rice husk and (b) composite of MCM-41 with rice husk prepared at 100 °C/24 h.

3.2. Adsorption isotherms

The type of adsorption isotherm model is very important in order to understand the adsorption behavior for solid–liquid adsorption system [32]. In the present study, Langmuir and Freundlich models, which are the most commonly used models, were applied to describe the adsorption behavior of phosphate. The Langmuir isotherm assumes that there is no significant interaction among adsorbed species and the adsorbent is saturated after the formation of monolayer of the active homogeneous sites within the adsorbent [33–35]. The Langmuir isotherm equation can be written as follows:

$$\frac{C_e}{q_e} = \frac{1}{bq_{max}} + \frac{C_e}{q_{max}} \quad (2)$$

where C_e is the equilibrium concentration of the remaining solute in the solution (mg/L), q_e is the amount of the phosphate adsorbed per mass unit of adsorbent at equilibrium (mg/g), q_{max} is the amount of adsorbate per mass unit of adsorbent at complete monolayer coverage (mg/g), and b is the Langmuir constant relating to the strength of adsorption (L/mg). If C_e/q_e is plotted against C_e, from the slope and intercept of this plot, q_{max} and b can be determined, respectively. The Langmuir adsorption isotherm for the removal of phosphate by rice husk composite with MCM-41 is shown in (Fig. 3). Linear plots of C_e/q_e versus C_e were found to be linear with a good correlation coefficient, $R^2 = 0.95$, indicated the applicability of Langmuir model in the present study. One of the essential characteristics of Langmuir isotherm could be expressed by a dimensionless constant called equilibrium parameter R_L which is determined as follows:

$$R_L = 1/(1 + bC_0) \quad (3)$$

where, b is a Langmuir constant and C_0 is the initial concentration. The value of R_L was calculated using the above expression. The values of R_L indicate the nature of the adsorption process [36].
$R_L > 1$ for unfavorable adsorption,
$R_L = 1$ for linear adsorption,
$0 < R_L < 1$ for favorable adsorption, and
$R_L = 0$ for irreversible adsorption.

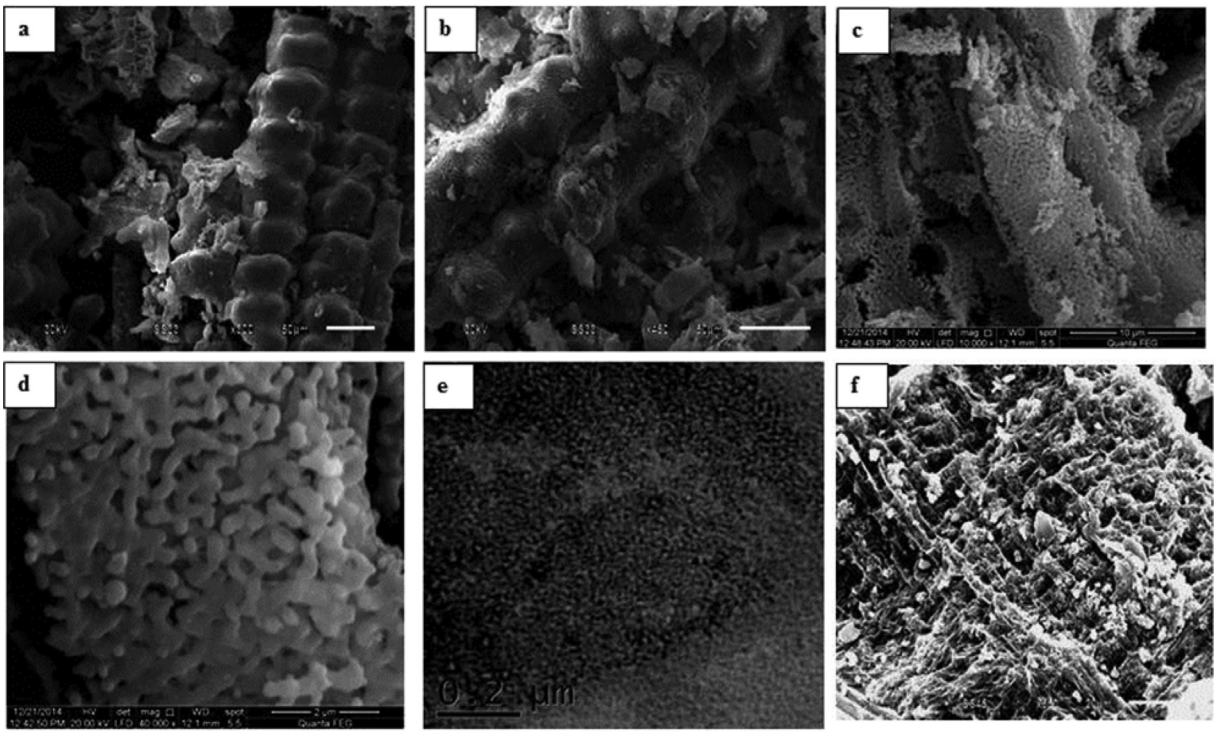

Fig. 2. SEM and TEM images of composite of MCM-41 with rice husk synthesized at 100 °C/24 h: MCM-41 silica on the surface of rice husk (a and b), aggregated particles of MCM-41(c and d) at different magnifications and TEM of composite of MCM-41 with rice husk (e) and SEM image after phosphate adsorption at 30 min of contact time (f).

The R_L-values for phosphate range from 0.69 to 0.92, indicating the adsorption process is favorable. The Freundlich isotherm model can be used to describe the non-ideal adsorption of a heterogeneous system and reversible adsorption [37]. According to this model, reactions take place in different sorption sites and as the amount of solute adsorbed rises, the binding surface energy decreases exponentially showing multilayer sorption [35]. The Freundlich isotherm is expressed as follows:

$$\log q_e = \log K_F + \frac{1}{n}\log C_e \quad (4)$$

where K_F and n are the Freundlich constants related to adsorption capacity and intensity, respectively. The values of K_F and $1/n$ are determined from the intercept and slope of the linear regressions. The $1/n$ value of Freundlich isotherm model for phosphate uptake by the synthetic MCM-41 silica with rice husk composite was 0.281 (i.e., less than unity) as shown in (Table 1), which refers to a heterogeneous surface with minimum interactions between the sorbed ions [35]. A plot of log (q_e) vs. log (C_e) for the studied samples is shown in (Fig. 4). Based on results obtained from the two applied models, the R^2 value for Langmuir isotherms (0.95) was higher than for Freundlich isotherm (0.54), indicating that the Langmuir model gave a better fit than the Freundlich model and therefore, adsorption of phosphate was a monolayer that takes place at specific homogeneous sites within composite of MCM-41 with rice husk.

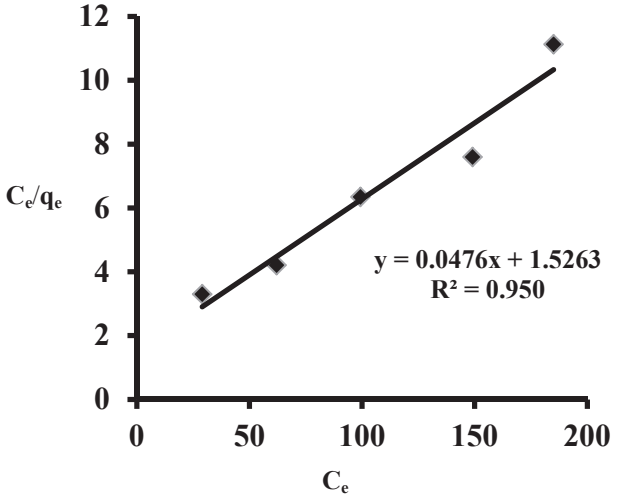

Fig. 3. Langmuir isotherm for phosphate uptake by composite of MCM-41 silica with rice husk.

3.3. Adsorption kinetics

The adsorption kinetics of phosphate onto composite of MCM-41 with rice husk after 5 m, 30 m, 2 h, 8 h and 24 h are given in (Fig. 5). As shown in Fig. 5, by increasing the shaking time from 5 min to 30 min, the amount of phosphate adsorbed increased from 11.35 mg/g to 14.92 mg/g. After 30 min, the removal amount of phosphate showed slight increased with values range from 15.32 mg/g to 15.39 mg/g to the end of shaking time, reaching a plateau, i.e. equilibrium was attained. Adsorption equilibrium might be due to the decrease in the available active adsorption sites

Table 1
Langmuir and Freundlich parameters for phosphate uptake by composite of MCM-41 silica with rice husk.

Isotherm model	Parameters	
Langmuir	q_{max} (mg/g)	21.01
	b (L/mg)	0.03
	R^2	0.95
Freundlich	$1/n$	0.218
	k	5.24
	R^2	0.545

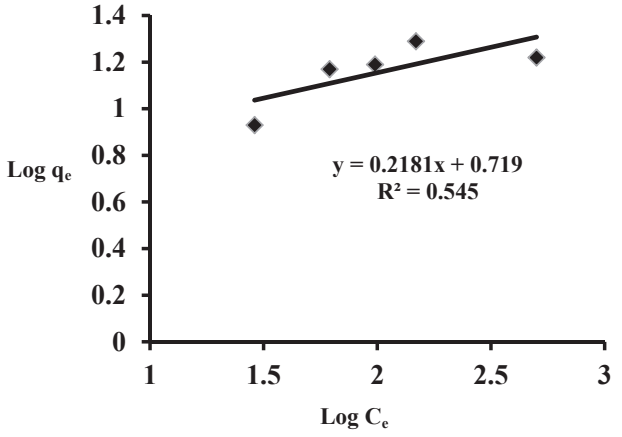

Fig. 4. Freundlich isotherm for phosphate uptake by composite of MCM-41 silica with rice husk.

on the adsorbent by increasing time followed by a decrease in limited mass transfer of the adsorbate molecules from the solution to the external surface of adsorbent [38].

In order to better understand the kinetics characteristics, Lagergren pseudo-second order kinetic model was applied in this study because it was found to be more likely to predict the behavior over the whole range of sorption [39]. This model is based on the assumption that the rate limiting step may be a chemical sorption occurring through sharing or exchange of electrons between the adsorbent and the adsorbate [40]. The pseudo-second order process can be written as follows:

$$\frac{t}{q_t} = \frac{1}{k_2 q_e^2} + \frac{t}{q_e} \tag{5}$$

where q_e is the equilibrium adsorption uptake (mg/g), q_t is the amount of phosphate adsorbed at time t (mg/g) and k_2 is the rate constant of second-order adsorption (g mg^{-1} min^{-1}). Thus, by plotting t/q_t versus t, k_2 and q_e values can be determined (Table 2). A good agreement of the experimental data with the second-order kinetic model was obtained (Fig. 6). The correlation coefficient is close to the unity, which suggests a strong relationship between the parameters and also explains the good applicability of the second order kinetic equation for phosphate adsorption by the synthetic composite of MCM-41 with rice husk. The adsorption process

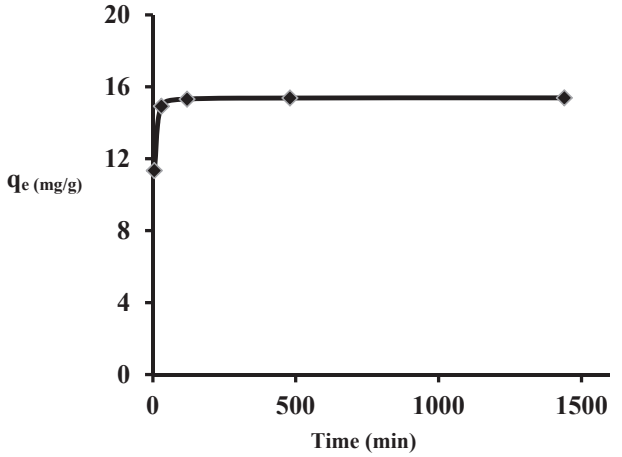

Fig. 5. Kinetics of phosphate uptake by composite of MCM-41 with rice husk.

Table 2
Parameters of pseudo-second order kinetics model.

Sorbent	k_2 (g/mg min)	q_e (cal) (mg/g)	R^2
Composite of MCM-41 silica with rice husk	6.9×10^{-2}	15.38	0.9999

involves transportation of the solute molecules from the aqueous solution to the surfaces of the solid particles followed by intra-particle diffusion/transport process [41]. The intra-particle diffusion can be written as follows:

$$q_t = k_p t^{1/2} + C \tag{6}$$

where k_p is the rate constant of intra-particle diffusion (mg g^{-1} $min^{-1/2}$) and was determined from the slopes of the lines in Fig. 7 and C is the intercept related to the thickness of the boundary layer. According to this model, if the plot of uptake, q_t, versus the square root of time, $t^{1/2}$ is linear and passes through the origin, then intra-particle diffusion is the only rate controlling step. As shown in Fig. 7, the plot does not pass through the origin and exhibited more than one step during the adsorption process. The first step was characterized by a steep slope due to the diffusion of phosphate ions onto the external surface of the synthetic material. The second stage showed a gentle slope indicating a gradual adsorption, where the intra-particle diffusion dominating throughout this stage. Therefore, the intra-particle diffusion is not only the rate limiting step in the whole adsorption process [42,34], as other processes might be involved.

3.4. Effect of adsorbent dosage

The effect of adsorbent mass on phosphate adsorption was studied by increasing the amount of adsorbent dose from 50 mg to 250 mg and the results are given in Fig. 8. By increasing the mass of adsorbent by 50, 100, 150 and 200 mg, the removal efficiency of phosphate increased by 36.5%, 64.13%, 68.87% and 73.35%, respectively. This was expected due to the increase in the number of active sites of adsorbent. By increasing the mass of adsorbent from 200 mg to 250 mg, the uptake efficiency increased little or none, i.e., from 73.35% to 73.42%. Thus, beyond 200 mg of the adsorbent mass, the % uptake of phosphate was nearly almost constant, which could be attributed the fact that upon increasing the adsorbent amount for the same concentration of phosphate ion (1 mM

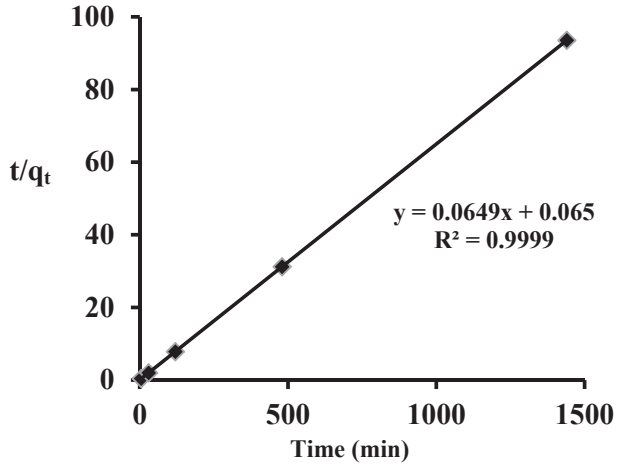

Fig. 6. Plots for second-order model for phosphate uptake by composite of MCM-41 with rice husk.

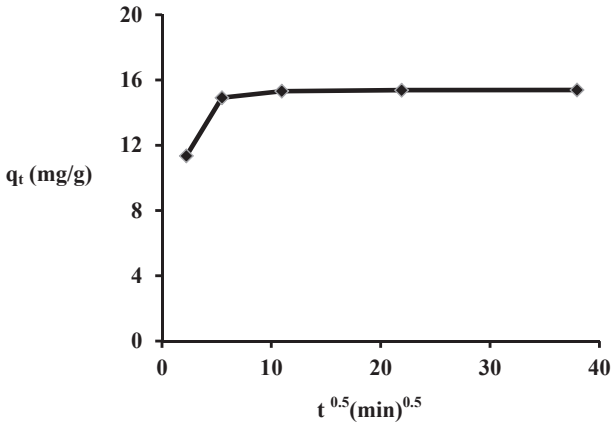

Fig. 7. Intraparticle diffusion model of phosphate adsorption by composite of MCM-41 silica with rice husk.

$Na_2HPO_4 \cdot 2H_2O$), the number of active sites available for the uptake of phosphate increases but a stage comes after which removal attains its maximum limit and further increase in dose had no effect as previously suggested [43]. However, further detailed studies may be necessary to explain this anomalous result.

3.5. Effect of pH on phosphate adsorption

Based on the fact that lower pH is favorable for the protonation of sorbent surface while at higher pH region, the negatively charged sites dominate. It is known that phosphate exists in different species, which include H_3PO_4, $H_2PO_4^-$, HPO_4^{2-} and PO_4^{3-} depending on solution pH ($pK_1 = 2.2$, $pK_2 = 7.2$, $pK_3 = 12.4$) [15]. The variation in the uptake of phosphate as a function of initial pH is shown in Fig. 9a and b. The highest amounts of phosphate uptake occurred at pH values ranging from 4.0 to 6.0, where the dominant phosphate species is the monovalent $H_2PO_4^-$. This may be related to the surface charge of the sorbent, which becomes positive at lower pH [13]. The presence of positive charges on the sorbent increase the attraction forces towards the negatively charged $H_2PO_4^-$ in the solution and therefore, led to an increase in the amount of the adsorption. By further decreasing the pH of the solution (about 2), the phosphate species occur in the neutral form as H_3PO_4, resulting in unfavorable sorption performance at lower pH solution [44]. On the other hand, by increasing the pH of the solution above 7, the surface of sorbent was characterized by the presence of negative charge sites which will exhibit strong

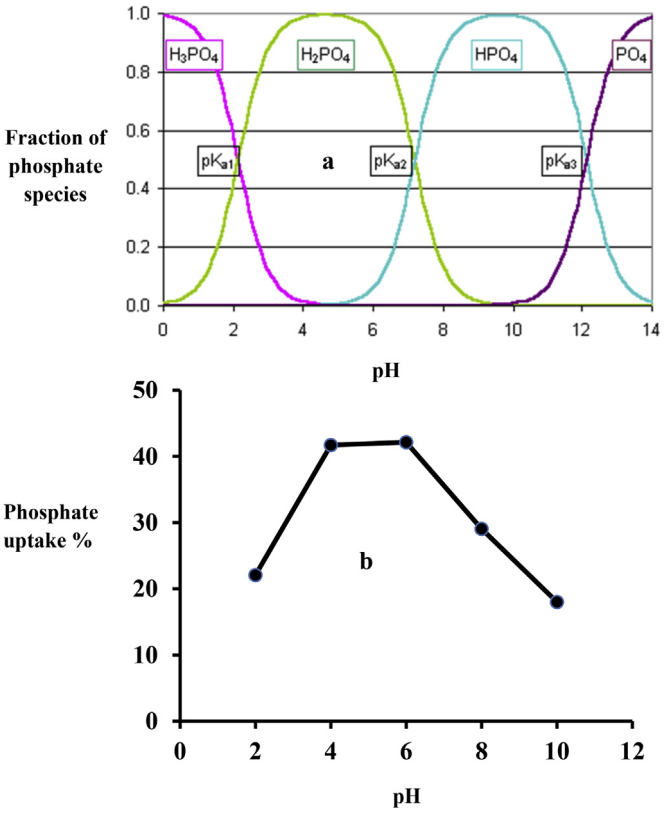

Fig. 9. Effect of pH on (a) fraction of phosphate species and (b) phosphate uptake by composite of MCM-41 silica with rice husk.

repulsive forces towards the phosphate species HPO_4^{2-} and PO_4^{3-} and therefore, the % uptake of phosphate decreased [45].

3.6. Effects of competitive anions and determination of K_d values

The effects of various competing anions such as SO_4^{2-}, NO_3^- and CO_3^{2-} on the uptake of phosphate by composite of MCM-41 with rice husk are shown in (Fig. 10). Various competing anions were used at 5× equivalent concentration of phosphate in order to determine phosphate selectivity. The amount of phosphate uptake decreased from 15.45 mg/g to 13.8 mg/g with the presence of sulfate anion. In the presence of NO_3^-, the adsorbed amount of phosphate decreased to 7.52 mg/g, which is about half the uptake when there was phosphate only in solution. On the other hand, the

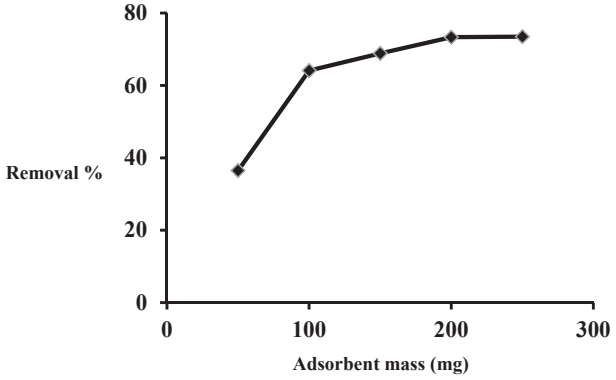

Fig. 8. The effect of adsorbent mass on phosphate adsorption by composite of MCM-41 silica with rice husk.

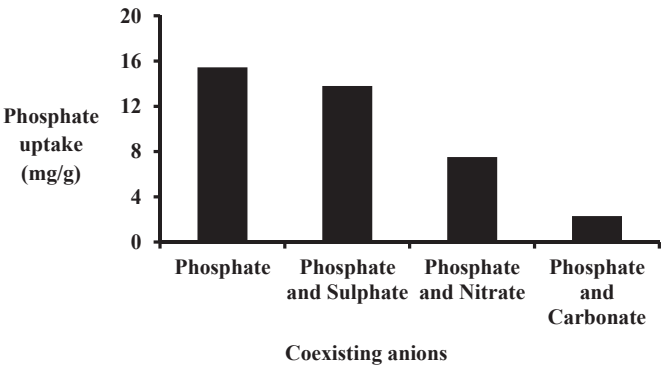

Fig. 10. Effect of add anions on phosphate uptake by composite of MCM-41 silica with rice husk (without keeping the initial pH constant).

Table 3
The effect of coexisting anions on pH and K_d values for the composite of MCM-41 silica with rice husk.

Matrix	Initial pH	Final pH	K_d (ml/g)
1 mM of sodium phosphate	6.15	6.53	121
1 mM of sodium phosphate + 5 mM of sodium sulfate	5.98	6.71	98
1 mM of sodium phosphate + 5 mM of sodium nitrate	9.52	9.63	48
1 mM of sodium phosphate + 5 mM of sodium carbonate	10.40	10.27	12

presence of CO_3^{2-} sharply decreased the amount of phosphate uptake with a value of 2.3 mg/g (Fig. 10). The presence of NO_3^- and CO_3^{2-} strongly affected the phosphate uptake that may be due to the initial pH of solutions which are 9.52 and 10.41 for nitrate and carbonate anions, respectively (Table 3). Similar results were obtained by determination of the K_d values where the higher K_d value (121 ml/g) was given by phosphate anion alone while the lower value (12 ml/g) was recorded by addition of CO_3^{2-} to phosphate anion (Table 3). Fig. 11 shows the effects of the investigated competing ions on the uptake of phosphate by composite of MCM-41 with rice husk by keeping the initial pH constant at 6. As shown in Fig. 11, no clear change was observed on the uptake of phosphate by the synthetic composite, especially with the presence of carbonate and nitrate anions as compared to the previous experiment which was carried out without keeping the initial pH constant. These results indicated that the selectivity of the synthetic rice husk composite with MCM-41 to phosphate is dependent on the pH of solution. In addition, rice husk composite with MCM-41 is highly selective to phosphate ion and therefore, suitable for the uptake of phosphate from aqueous solutions.

4. Conclusions

Composite of MCM-41 silica with rice husk synthesized under hydrothermal conditions showed large uptake capacity for phosphate removal and the maximum uptake capacity (Q_{max}) was 21.01 mg/g. The kinetics of phosphate uptake was fast and equilibrium was achieved after 30 min. The phosphate uptake was highly dependent on pH of the solution and the best removal efficiency was obtained at pH 6. The adsorption isotherms and kinetics characteristics are well described by Langmuir equation and pseudo-second order model, respectively. The study has also shown that phosphate uptake would be affected by the presence of high concentrations nitrate and carbonate as coexisting anions without keeping a constant initial pH. Rice husk composite with MCM-41 was found to be highly selective to phosphate ion and hence it is expected to be suitable for the uptake of phosphate from solutions by adjusting the pH to 6.

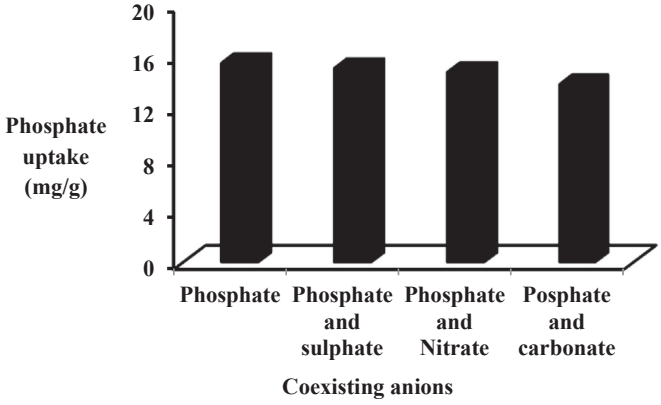

Fig. 11. Effect of add anions on phosphate uptake by composites of MCM-41 silica with rice husk (with keeping a constant pH at 6).

Acknowledgments

The authors thank the support unit and project finance, Beni-Suef University, Egypt for financially supporting this study.

References

[1] L. Zhang, L. Wan, N. Chang, J. Liu, C. Duan, Q. Zhou, X. Li, X. Wang, J. Hazard. Mater. 190 (2011) 848–855.
[2] X. Huang, X. Liao, B. Shi, J. Hazard. Mater. 166 (2009) 1261–1265.
[3] X. Song, Y. Pan, Q. Wu, Z. Cheng, W. Ma, Desalination 280 (2011) 384–390.
[4] Y. Zhao, L. Zhang, F. Ni, B. Xi, X. Xia, X. Peng, Z. Luan, Desalination 273 (2011) 414–420.
[5] M. Zamparas, A. Gianni, P. Stathi, Y. Deligiannakis, I. Zacharias, Appl. Clay Sci. 62–63 (2012) 101–106.
[6] M.A. Ahmed, A.I.M. Aly, R.A. Hussein, Arab. J. Nucl. Sci. Appl. 46 (2013) 1–17.
[7] M.A.H. Saad, Water Air Soil Pollut. 2 (1973) 522–525.
[8] K. Karageorgiou, M. Paschalis, G. Anastassakis, J. Hazard. Mater. A139 to 139 (2007) 447–452.
[9] H. Yin, Y. Yun, Y. Zhang, C. Fan, J. Hazard. Mater. 198 (2011) 362–369.
[10] M.W. Kamiyango, W.R.L. Masamba, S.M.I. Sajidu, E. Fabiano, Phys. Chem. Earth 34 (2009) 850–856.
[11] F. Gan, J. Zhou, H. Wang, C. Du, X. Chen, Water Res. 43 (2009) 2907–2915.
[12] N. Hamdi, E. Srasra, J. Environ. Sci. 24 (4) (2012) 617–623.
[13] M.Y. Can, E. Yildiz, J. Hazard. Mater. B135 to 135 (2006) 165–170.
[14] M. Zhang, B. Gao, Y. Yao, Y. Xue, M. Inyang, Chem. Eng. J. 210 (2012) 26–32.
[15] R. Saad, K. Belkacemi, S. Hamoudi, J. Colloid Interface Sci. 311 (2007) 375–381.
[16] Z. Jia, Q. Wang, J. Liu, L. Xu, R. Zhu, Colloids Surf. A Physico. Eng. Asp. 436 (2013) 495–503.
[17] K.A. Krishnan, A. Haridas, J. Hazard. Mater. 152 (2008) 527–535.
[18] E. Zong, D. Wei, H. Wan, S. Zheng, Z. Xu, D. Zhu, Chem. Eng. J. 221 (2013) 193–203.
[19] T. Kasama, Y. Watanabe, H. Yamada, T. Murakami, Appl. Clay Sci. 25 (2004) 167–177.
[20] A. Halajnia, S. Oustan, N. Najafi, A.R. Khataee, A. Lakzian, Appl. Clay Sci. 80–81 (2013) 305–312.
[21] R. Siddique, Waste Materials and By-product in Concrete, Springer-Verlag Berlin Heidelberg, 2008.
[22] P.M. Yeletsky, V.A. Yakovlev, M.S. Mel'gunov, V.N. Parmon, Microporous Mesoporous Mater. 121 (2009) 34–40.
[23] I.O. Ali, A.M. Hassan, S.M. Shaaban, K.S. Soliman, Sep. Purif. Technol. 83 (2011) 38–44.
[24] H. Katsuki, S. Furuta, T. Watari, S. Komarneni, Microporous Mesoporous Mater. 86 (2005) 145–151.
[25] Y. Cheng, M. Lu, J. Li, X. Su, S. Pan, C. Jiao, M. Feng, J. Colloid Interface Sci. 369 (2012) 388–394.
[26] S. Kumagai, H. Ishizawa, Y. Aoki, Y. Toida, Chem. Eng. J. 156 (2010) 270–277.
[27] H. Katsuki, S. Komarneni, J. Solid State Chem. 182 (2009) 1749–1753.
[28] M.K. Seliem, S. Komarneni, R. Parette, H. Katsuki, F.S. Cannon, M.G. Shahien, A.A. Khalil, I.M. Abd El-Gaid, Mater. Res. Innov. 14 (2010) 351–354.
[29] M.K. Seliem, S. Komarneni, R. Parette, H. Katsuki, F.S. Cannon, M.G. Shahien, A.A. Khalil, I.M. Abd El-Gaid, Appl. Clay Sci. 53 (2011) 621–626.
[30] M.S. Masoud, W.M. El-Saraf, A.M. Abdel-Halim, A.E. Ali, E.A. Mohamed, H.M.I. Hassan, Arab. J. Chem. (2012) 1–7.
[31] K. Grover, S. Komarneni, H. Katsuki, Appl. Clay Sci. 48 (2010) 631–637.
[32] X. Han, W. Wang, X. Ma, Chem. Eng. J. 171 (2011) 1–8.
[33] N. Hoda, E. Bayram, E. Ayranci, J. Hazard. Mater. B137 to 137 (2006) 344–351.
[34] M.K. Seliem, S. Komarneni, T. Byrne, F.S. Cannon, M.G. Shahien, A.A. Khalil, I.M. Abd El-Gaid, Appl. Clay Sci. 71 (2013) 21–26.
[35] S. Bagherifam, S. Komarneni, A. Lakzianb, A. Fotovat, R. Khorasani, W. Huang, J. Ma, S. Hong, F.S. Cannon, Y. Wang, Appl. Clay Sci. 95 (2014) 126–132.
[36] L. Lian, L. Guo, C. Guo, J. Hazard. Mater. 161 (2009) 126–131.
[37] S. Wang, Z.H. Zhu, J. Hazard. Mater. B136 to 136 (2006) 946–952.
[38] S. Mehdizadeh, S. Sadjadi, S.J. Ahmadi, M. Outokesh, J. Environ. Health Sci. Eng. 12 (2014) 1–7.
[39] M. Kragovic, A. Dakovic, M. Markovic, J. Krstic, G.D. Gatta, Appl. Surf. Sci. 283 (2013) 764–774.
[40] K.S. Hui, C.Y.H. Chao, S.C. Kot, J. Hazard. Mater. B127 to 127 (2005) 89–101.
[41] H. Demiral, G. Gunduzoglu, Bioresour. Technol. 101 (2010) 1675–1680.
[42] R. Katal, M.S. Baei, H.T. Rahati, H. Esfandian, J. Ind. Eng. Chem. 18 (2012) 295–302.
[43] M. Kapur, M.K. Mondal, J. Taiwan Inst. Chem. Eng. 45 (2014) 1803–1813.
[44] Q. Zhang, Q. Du, T. Jiao, B. Pan, Z. Zhang, Q. Sun, S. Wang, T. Wang, F. Gao, Chem. Eng. J. 221 (2013) 315–321.
[45] G. Zhang, H. Liu, R. Liu, J. Qu, J. Colloid Interface Sci. 335 (2009) 168–174.